Studying small-scale magnetic features in the quiet Sun

Fatima Kahil

Max Planck Institute for Solar System Research-Göttingen, Germany
Solar Lower Atmosphere and Magnetism

S. Solanki & T. Riethmüller

May 10, 2016

Introduction - Magnetic elements

- Enhanced brightness (continuum+spectral lines) with respect to surroundings
- Concentrated in the dark intergranular lanes.
- Described by vertical flux tubes.
    - Magnetic pressure $\rightarrow$ reduce in p_i $\rightarrow$ internal evacuation
    - Buoyancy $\rightarrow$ vertical flux tube
    - Opacity depression: shift of $\tau = 1$ level $\rightarrow$ brightening with respect to surroundings
    - Expansion with height: flux conservation inside the flux-tube $\Rightarrow$ "Wine-glass" shape

- $\boxed{p_e = p_i + B^2/8\pi}$

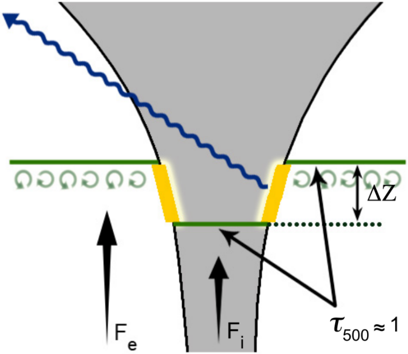

Introduction - Magnetic elements

- Contribution of magnetic elements to the TSI variations over the solar cycle: 30% at continumm wavelengths, and 60% at wavelengths below 400 nm (Krivova et al. 2006)
- Chromospheric structuring and heating of the outer atmosphere.

Visible continuum contrast vs. B_{LOS}

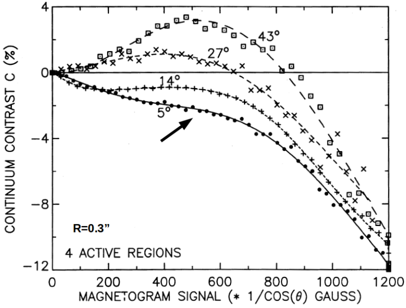

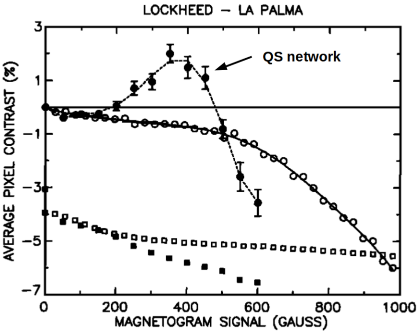

Figure : Topka et al.(1992); Lawrence et al.(1993)

Visible continuum contrast vs. B_{LOS}

Hinode/SP (0.3"): Fe I 630.15 nm and 630.25 nm lines

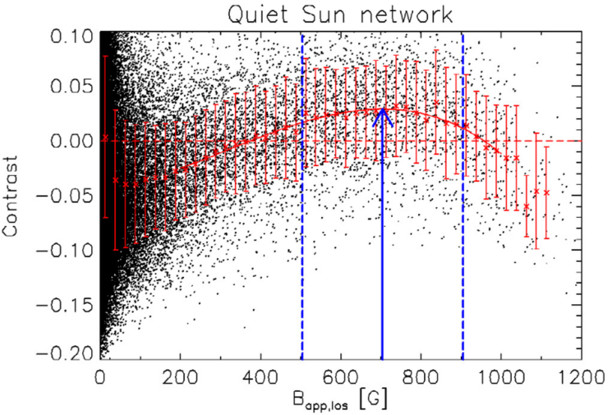

Figure : Kobel et al.(2011)

Visible continuum contrast vs. B_{LOS}

Hinode/SP (0.3"): Fe I 630.15 nm and 630.25 nm lines

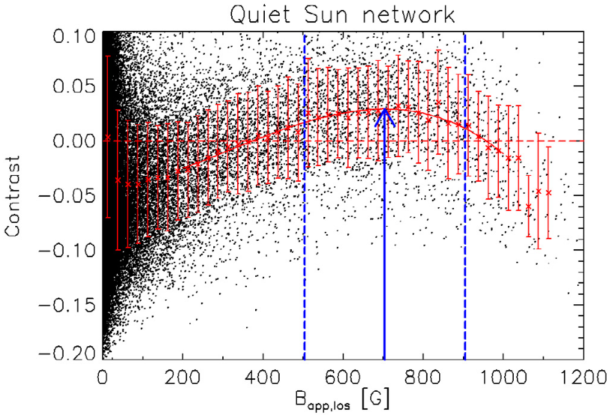

Figure : Kobel et al.(2011)

- Pores excluded!

Visible continuum contrast vs. B_{LOS}

Hinode/SP (0.3"): Fe I 630.15 nm and 630.25 nm lines

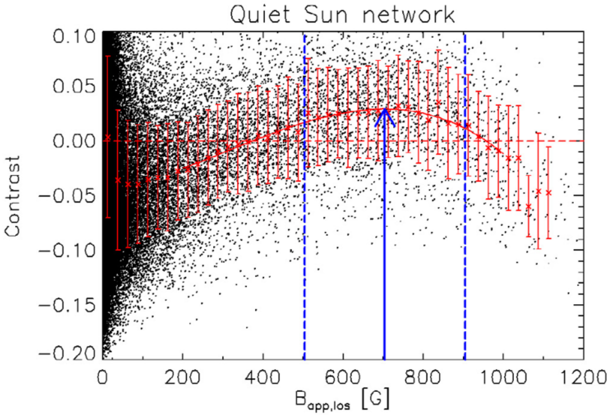

Figure : Kobel et al.(2011)

- Pores excluded!
- spatial resolution?

Aims & Motivation

- Balloon-borne solar observatory: 1 m telescope/UV filter imager/imaging vector polarimeter (@ $\sim$ 37 km)
- Diffraction limited angular resolution: 0.05" (35 km) at 214 nm, and 0.1"(70 km) in the visible.
- High angular, temporal, and spectral resolution observations, in the visible and UV down to 200 nm.

Aims & Motivation

- Balloon-borne solar observatory: 1 m telescope/UV filter imager/imaging vector polarimeter (@ $\sim$ 37 km)
- Diffraction limited angular resolution: 0.05" (35 km) at 214 nm, and 0.1"(70 km) in the visible.
- High angular, temporal, and spectral resolution observations, in the visible and UV down to 200 nm.

Aims

- Relationship between the brightness in the continuum and NUV, with B_{los}
- Relationship between the lower chromosphere emission and B_{los}
- Constrain radiative MHD simulations of flux tube models

Data Preparation - Image alignment

- Sufi at 214 nm, 300 nm, 313 nm, and 388 mm with IMaX Stokes I continuum at 525.02 nm.
- Sufi at 397 nm (core of CaII H) with IMaX stokes I line core
- Resampling to the same pixel size (IMaX's 0.05"/pixel)
- Cross-Correlation technique to find IMaX-SuFI offsets to a sub-pixel accuracy $\Longrightarrow$ Common FOV between all images ($13'' \times 38''$)

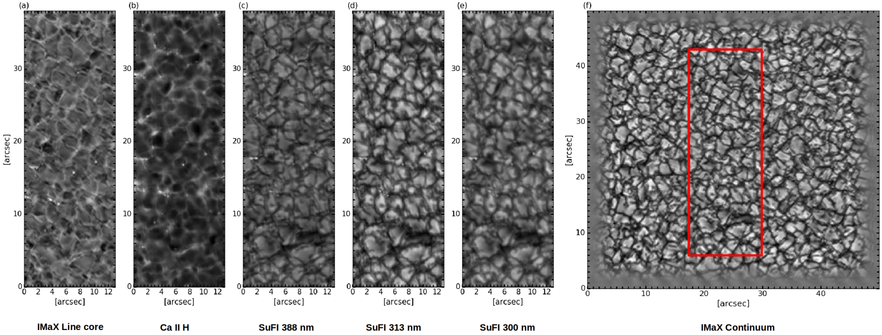

Visible continuum and line core contrasts

- brightness measured with respect to the mean continuum quiet Sun intensities $I_{cont,qs}$

$$C_{cont} = \frac{I_{cont}}{I_{cont,qs}}$$

NUV contrasts

- $I_{NUV,qs}$ is the average intensity for pixels with $B_{los} \leq 2\sigma$

$$C_{NUV} = \frac{I_{NUV}}{I_{NUV,qs}}$$

Visible continuum contrast vs. B_{LOS}

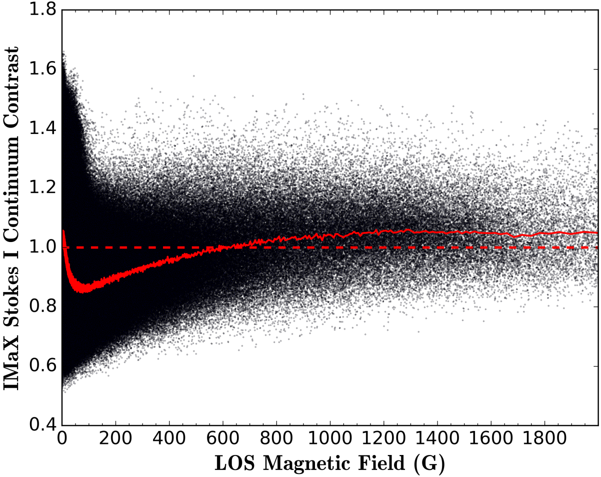

Figure : IMaX (0.15"/Fe I 525.04 nm), Kahil et al.(2016, in preparation)

Visible continuum contrast vs. B_{LOS}

- granulation: $B \approx 0$
- field concentration in integranular lanes ($B \geq 70\ G$)
- network region

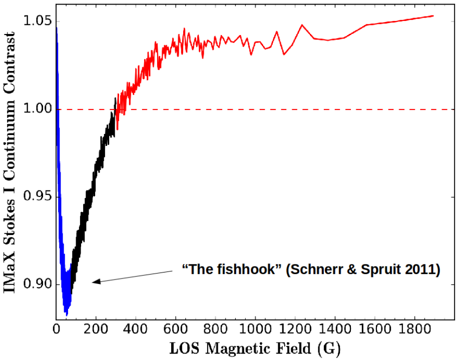

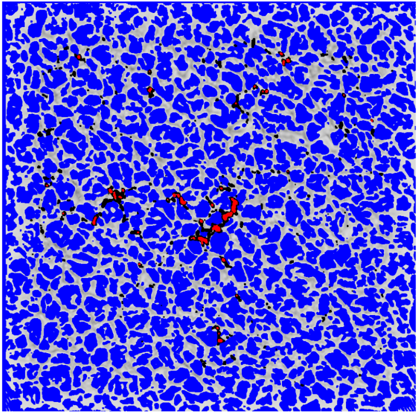

Visible continuum contrast vs. B_{LOS}

- Stokes I and V convolved with a gaussian of FWHM = 0.32"
- B_{los} derived from C-O-G
  - $B_{max} \approx 470$ G (with stray-light)
  - $B_{max} \approx 665$ G (corrected for stray-light)

Visible continuum contrast vs. B_{LOS}

- Stokes I and V convolved with a gaussian of FWHM = 0.32"
- B_{los} derived from C-O-G
  - $B_{max} \approx 470$ G (with stray-light)
  - $B_{max} \approx 665$ G (corrected for stray-light)

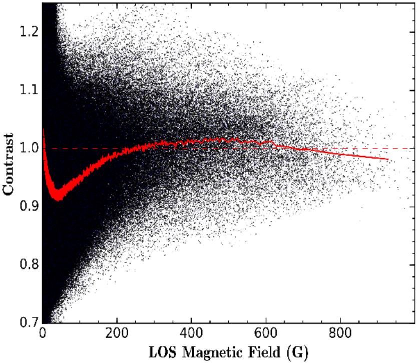

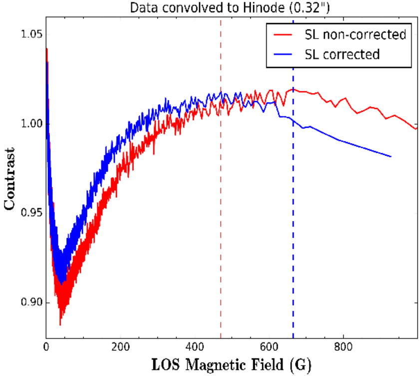

Chromospheric emission vs. photospheric magnetic field

- QS is responsible for the heating of the outer chromosphere.
- Ca II-H line: chromospheric diagnostic

author	b	comments
Schrijver et al.(1989)	0.66	Mount Wislon (AR's)
Ortiz and Rast(2005)	0.6	SOHO/MDI (QS)
Rezai et al.(2007)	0.2	VTT (QS N+IN)
Loukitcheva et al.(2009)	0.31	BBSO+SOHO/MDI (time averaged data)

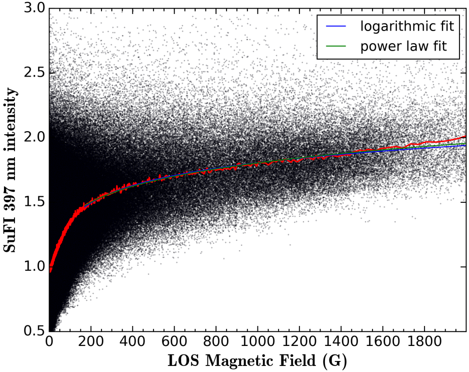

$$\boxed{I = a.B^b + I_0} \quad (1) \qquad I_0\text{: basal flux}$$

$$\boxed{I = a'.\log_{10}(B) + b'} \quad (2)$$

cut(G)	b	χ^2 (1)	χ^2 (2)
170	0.14±0.02	1.03	1.2
190	0.18±0.02	0.94	1.17
210	0.21±0.02	0.90	1.12
230	0.25±0.03	0.84	1.10
250	0.33±0.03	0.73	1.07

UV brightness vs. photospheric magnetic field

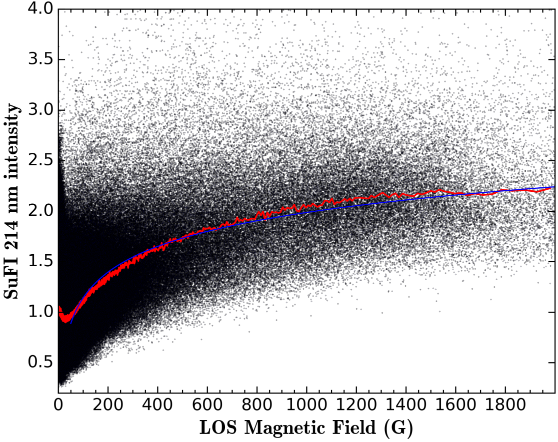

$$\boxed{\frac{I}{<I_{qs}>} = a.\log_{10}(B) + b}$$

cut(G)	a	b	χ^2
90	0.93±0.003	-0.77±0.008	2.33
100	0.94±0.003	-0.80±0.008	1.93
150	0.97±0.004	-0.88±0.01	1.18
200	0.97±0.006	-0.90±0.01	0.99
250	0.97±0.006	-0.88±0.02	0.88

NUV brightness vs. photospheric magnetic field

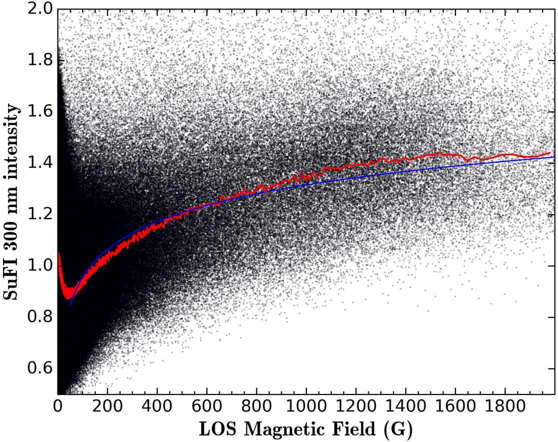

$$\boxed{\frac{I}{<I_{qs}>} = a.\log_{10}(B) + b}$$

cut(G)	a	b	χ^2
90	0.41±0.002	0.09±0.005	3.34
100	0.42±0.002	0.07±0.005	2.70
150	0.44±0.002	0.01±0.006	1.33
200	0.45±0.002	-0.03±0.007	0.93
250	0.46±0.003	-0.04±0.009	0.82

NUV brightness vs. photospheric magnetic field

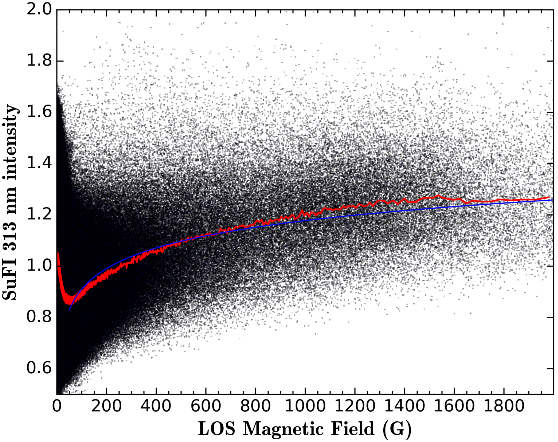

$$\frac{I}{<I_{qs}>} = a.\log_{10}(B) + b$$

cut(G)	a	b	χ^2
90	0.31±0.001	0.26±0.003	2.66
100	0.31±0.002	0.25±0.004	2.12
150	0.33±0.002	0.20±0.004	1.10
200	0.34±0.002	0.18±0.005	0.84
250	0.34±0.002	0.17±0.007	0.74

NUV brightness vs. photospheric magnetic field

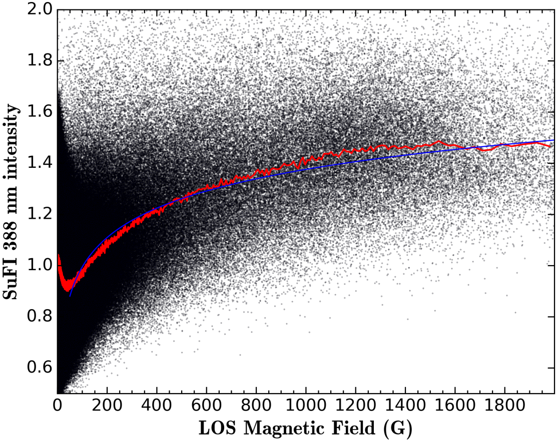

$$\boxed{\frac{I}{<I_{qs}>} = a.\log_{10}(B) + b}$$

cut(G)	a	b	χ^2
90	0.43±0.002	0.11±0.004	2.62
100	0.43±0.002	0.09±0.004	2.17
150	0.45±0.002	0.05±0.006	1.53
200	0.45±0.003	0.04±0.008	1.34
250	0.45±0.004	0.04±0.01	1.26

MHD simulations

- Röhrbein et al.(2011):
  - MURaM code: plage region ($B = 200$ G)
  - convolution with Airy functions of $D = 1.0$ m (Sunrise) and $D = 0.5$ cm (Hinode)
  - $\lambda = 630.2$ nm

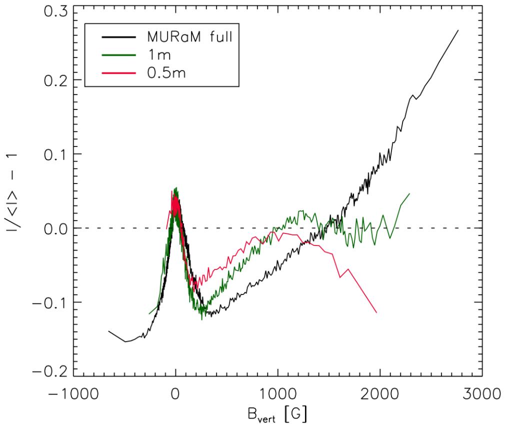

C-O-G vs Inversions

- C-O-G applied on stray-light corrected stokes profiles (lev2.3)
  Center of gravity method (Rees & Semel 1979):

$$\lambda_{\pm} = \frac{\int_{-\infty}^{+\infty} \Delta\lambda [I_c - (I \pm V)] d\Delta\lambda}{\int_{-\infty}^{+\infty} (I_c - (I \pm V)) d\Delta\lambda}$$

$$B_{LOS} = \frac{|\Delta\lambda_Z|}{C_0 \times g \times \lambda_0^2}, \quad \Delta\lambda_Z = \frac{\lambda_+ - \lambda_-}{2}$$

$$\Delta\lambda_G = \frac{\int_{-\infty}^{+\infty} V \Delta\lambda d\Delta\lambda}{\int_{-\infty}^{+\infty} (I_c - I) d\Delta\lambda}$$

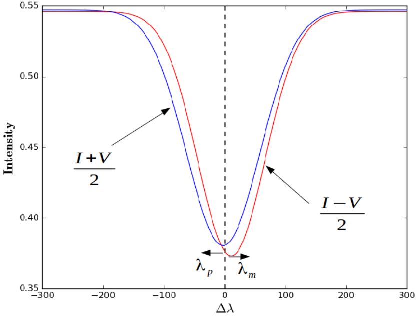

C-O-G vs Inversions

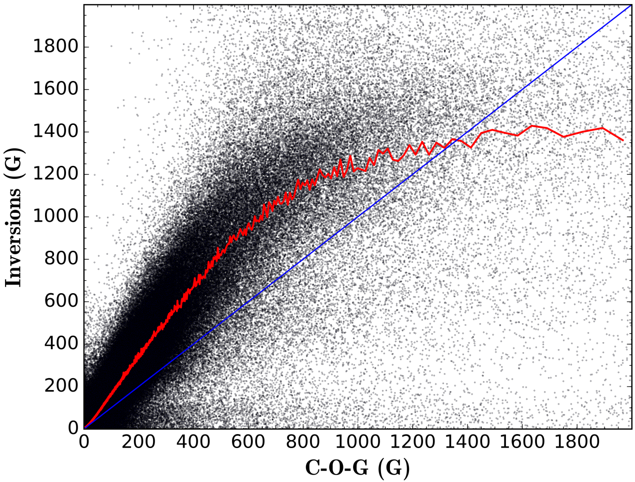

Figure : B_{los} derived from inversions vs. B_{los} from C-O-G on IMaX data points

C-O-G vs Inversions

Lower horizontal branch

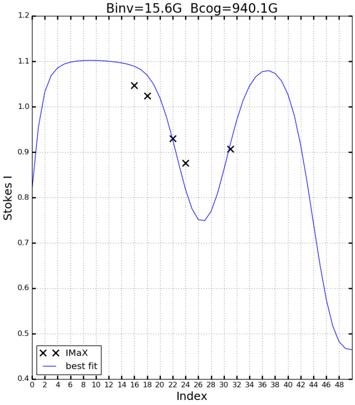

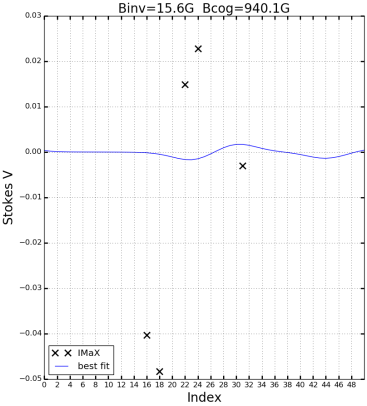

C-O-G vs Inversions

Lower horizontal branch

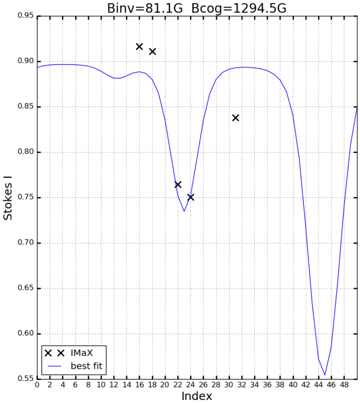

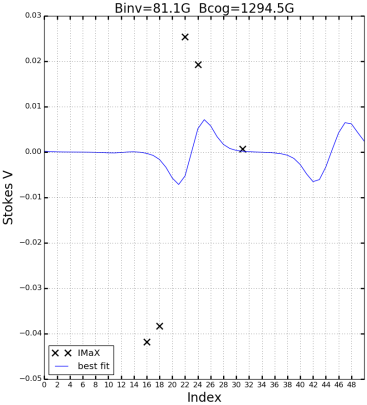

C-O-G vs Inversions

Lower horizontal branch

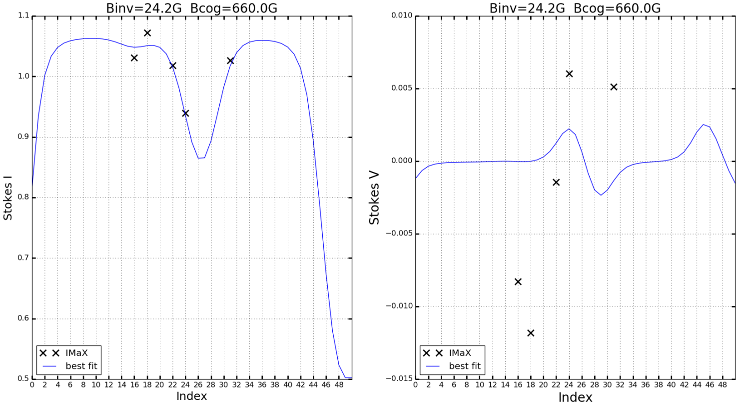

C-O-G vs Inversions

Linear slope

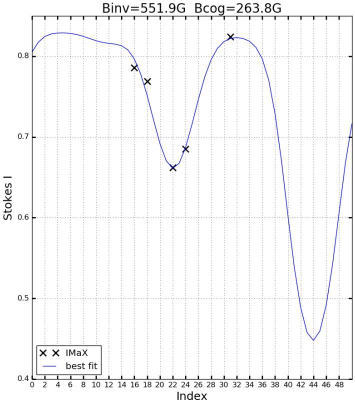

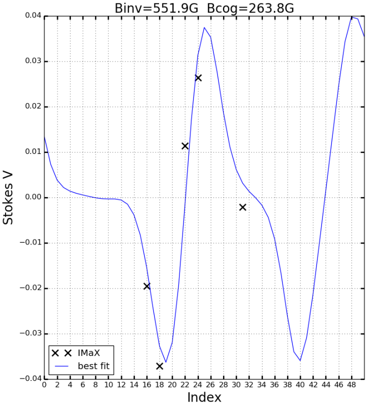

C-O-G vs Inversions

Linear slope

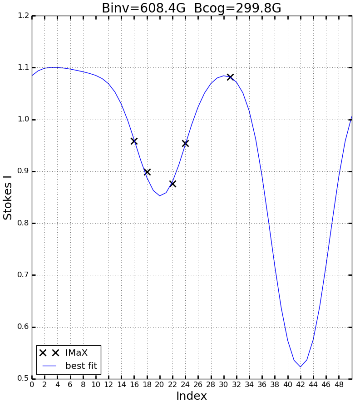

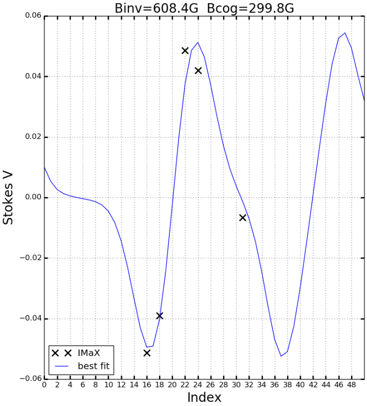

Linear slope

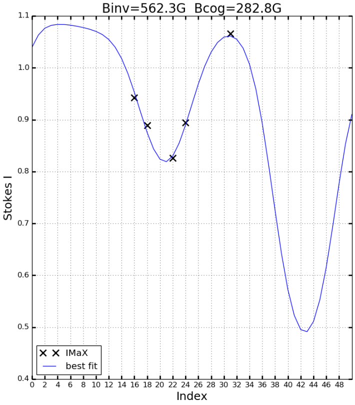

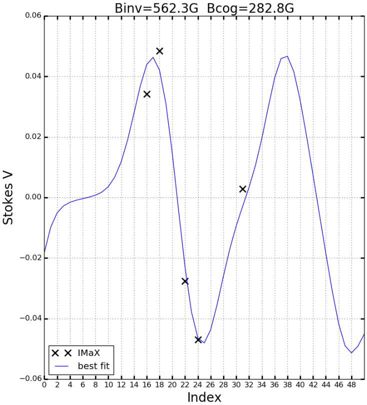

C-O-G vs Inversions

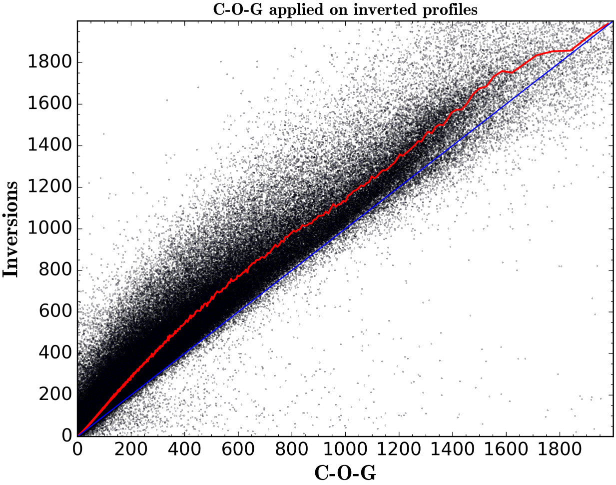

Figure : B_{los} derived from inversions vs. B_{los} from C-O-G on inverted profiles

Future Projects

- Granulation properties (velocity, size, lifetime..) in the quiet Sun inferred from IMaX and SuFI, and comparison to MHD simulations.
- CLV of continuum and UV contrasts vs B_{los} of small-scale features.
- Continuum and UV brightness of plage regions (Sunrise2) vs B_{los} , and comparison with MHD simulations.
- Photospheric magnetic fields determination techniques and approximations (C-O-G, weak-field, Inversions).
- Signatures of magnetic reconnection processes in the quiet Sun.

Thank you!